Ocean Modelling 79 (2014) 33–42

Contents lists available at ScienceDirect

Ocean Modelling

journal homepage: www.elsevier.com/locate/ocemod

Is realistic Antarctic sea-ice extent in climate models the result of excessive ice drift?

P. Uotila [a,b,*], P.R. Holland [c], T. Vihma [b], S.J. Marsland [a], N. Kimura [d]

[a] CSIRO-Marine & Atmospheric Research, Aspendale, Australia
[b] Finnish Meteorological Institute, Helsinki, Finland
[c] British Antarctic Survey, Cambridge, UK
[d] National Institute of Polar Research, Tachikawa, Japan

ARTICLE INFO

Article history:
Received 28 October 2013
Received in revised form 10 April 2014
Accepted 21 April 2014
Available online 2 May 2014

Keywords:
Thermodynamics
Divergence
Advection

ABSTRACT

For the first time, we compute the sea-ice concentration budget of a fully coupled climate model, the Australian ACCESS model, in order to assess its realism in simulating the autumn–winter evolution of Antarctic sea ice. The sea-ice concentration budget consists of the local change, advection and divergence, and the residual component which represents the net effect of thermodynamics and ridging. Although the model simulates the evolution of sea-ice area reasonably well, its sea-ice concentration budget significantly deviates from the observed one. The modelled sea-ice budget components deviate from observed close to the Antarctic coast, where the modelled ice motion is more convergent, and near the ice edge, where the modelled ice is advected faster than observed due to inconsistencies between ice velocities. In the central ice pack the agreement between the model and observations is better. Based on this, we propose that efforts to simulate the observed Antarctic sea-ice trends should focus on improving the realism of modelled ice drift.

1. Introduction

The Antarctic sea ice is expanding and climate models have difficulties in simulating this trend (Turner et al., 2013a), for yet unknown reasons. A small number of climate model simulations, however, show a similar increase of Antarctic sea-ice extent to the observed one which may indicate that the internal variability of the climate system, rather than forcing due to greenhouse gas concentrations, plays a significant role (Zunz et al., 2013). This hypothesis is supported by Mahlstein et al. (2013), who studied Antarctic sea-ice area derived from a large ensemble of 23 climate models and found that the internal sea-ice variability is large in the Antarctic region indicating that both the observed and modelled trends can represent natural variations along with external forcings. Moreover, Polvani (2013) analysed forced and preindustrial control model simulations of four climate models to see whether their Antarctic sea-ice trends are due to the internal variability or not. They found that the observed Antarctic trend falls within the distribution of trends arising naturally from the coupled atmosphere–ocean–sea-ice system and concluded that it is difficult to attribute the observed trends to anthropogenic forcings. Consistent with Polvani (2013) and Swart and Fyfe (2013) show that when accounting for internal variability, an average multi-model sea-ice area trend is statistically compatible with the observed trend.

However, the validity of the hypothesis that the Antarctic sea-ice increase is due to the internal variability of the climate system remains uncertain because the models used to test the hypothesis show biases in the mean state and regional patterns, and overestimate the interannual variance of sea-ice extent, particularly in winter (Zunz et al., 2013). To confirm the argument of natural variability, a model would have to explain the observed sea-ice increase while simultaneously responding to anthropogenic forcings. Hence, it appears that the models can not be used to test precisely whether the observed sea ice expansion is due to the internal variability of the climate system or not.

In addition to the above mentioned model based studies, a recent observational study supports to some extent the argument of internal variability. Meier et. al (2013) analysed satellite data and showed that the Antarctic sea-ice extent in 1964 was larger than anytime during 1979–2012. This is a robust result, because within the wide range of uncertainty in the 1964 satellite estimate, the 1964 ice extent is higher than the monthly September average of any of the years of the satellite record from 1979–2012 and remains on the highest end of the estimates even when taking into

* Corresponding author at: Finnish Meteorological Institute, Helsinki, Finland.
E-mail address: petteri.uotila@fmi.fi (P. Uotila).

http://dx.doi.org/10.1016/j.ocemod.2014.04.004
1463-5003/

consideration the variation within the month. According to Meier et. al (2013), the ice cover may currently be recovering from a relatively low level back to higher conditions seen in the 1960s. Hence, this result suggests that the current 33 year increase in the sea-ice extent is due to the long-term variability of the climate system. Whether this long-term variability is only due to the internal variability or due to the combined effects of forcings and the internal variability remains unclear.

Observations can also be used to show that the Antarctic sea-ice concentration trends are closely associated with trends in ice drift or with trends related to thermodynamics (Holland and Kwok, 2012). The observed Antarctic sea-ice drift trends can be explained by changes in local winds and the aspects of local winds can be attributed to large-scale atmospheric circulation modes (Uotila et al., 2013b), which have experienced significant changes in the last thirty years (Solomon et al., 2007, Turner et al., 2013b). Moreover, Holland and Kwok (2012) show where the evolution of Antarctic sea ice is controlled either by thermodynamic or dynamic processes during its autumnal expansion and in winter. This is particularly valuable because the relatively weak overall Antarctic sea-ice trend consists of strong regional but opposing trends (Turner et al., 2009). Holland and Kwok (2012) suggest that, by comparing their observational results with similarly processed climate model output, one can diagnose faults in a climate model due to thermodynamic or dynamic processes when simulating the Antarctic sea ice. This is the motivation of our study — to investigate whether a fully coupled climate model produces realistic contributions from thermodynamic and dynamic sea-ice evolution. In this way we should be able to address which processes in the model are too poorly represented to realistically simulate the currently observed sea-ice state, its variability and its trends. Results from such an analysis have not yet been published.

Related to this, recent studies have shown that coupled ocean–ice models, where atmospheric states are prescribed, can reproduce observed Antarctic sea-ice trends under realistic atmospheric forcing and/or when they are constrained with observations. Massonnet et al. (2013) assimilated sea-ice concentration into an ocean–ice model to generate Antarctic sea-ice volume time series from 1980–2008. Additionally, Zhang (2013) shows by an ocean–ice model that intensifying winds result in increase in sea-ice speed, convergence and sea-ice deformation. The sea-ice deformation increases the volume of thick ice in the ocean–ice model along with a significant sea-ice concentration increase in the Southern Weddell Sea. Importantly, Holland et al. (2014) show that a free-running ocean–ice model forced by atmospheric re-analyses can reproduce Antarctic sea-ice concentration and drift trends as observed. Hence, atmospheric states of a fully coupled climate model seem crucial for the modelled sea-ice trends. Accordingly, an assessment of the thermodynamic and dynamic processes related to the evolution of sea-ice concentration in a fully coupled climate model is an important next step to understand why climate models have not been able to simulate Antarctic sea ice realistically.

We hypothesise that climate models simulate the seasonal evolution of integrated Antarctic sea-ice area, and integrated extent, reasonably well, even with relatively unrealistic dynamic and thermodynamic components of the sea-ice concentration budget, partly due to the balancing of biases of these components. For example, during its autumnal expansion sea ice is advected over a larger area when its speed is higher, but at the same time it melts more at the northernmost ice edge where the ocean and atmosphere are warm and the thermodynamics limits the dynamical expansion of sea ice. In order to produce observed regional sea-ice concentration trends in decadal time scales, and the overall sea-ice area or extent trends for the right reasons, and therefore with the correct mass, energy and momentum fluxes, climate models need to simulate regional dynamical and thermodynamical processes correctly.

To test the success of our hypothesis, we compare modelled dynamic and thermodynamic components of the Antarctic April–October sea-ice concentration budget as derived from the output of a well performing state-of-the-science climate model with the observed budget of Holland and Kwok (2012). The observed sea-ice concentration budget data of Holland and Kwok (2012) is only available from April to October which limits our analysis to these months. We present the models, methods and data used for this analysis in the next section. In the results and discussion section, we compare modelled sea-ice concentration budgets with observed ones and discuss how their differences affect the sea-ice evolution. Finally, in the last section we present the main conclusions of this study along with their implications.

2. Methods and data

We analyse data from four *historical* and one *rcp85* realisation simulated by the Australian Community Climate and Earth-System Simulator coupled model version 1.0 (ACCESS1.0) and 1.3 (ACCESS1.3) as submitted to the phase five of the Coupled Model Inter-comparison project (CMIP5) database Table 1, Fig. 1 and Dix et al. (2013). ACCESS1.0 and ACCESS1.3 differ in two important aspects: their sea-ice albedos are different and their atmospheric cloud microphysics schemes are different. Both these differences can be expected to affect the sea-ice performance. Therefore we wanted to see how much their sea-ice concentration budgets differ. The ACCESS configurations are one of the better performing CMIP5 models in terms of global sea-ice extent with a climatology relatively close to the observed one (Uotila et al., 2013a; Liu et al., 2013), thus justifying its selection for this study.

Moreover, similar analysis as for the ACCESS coupled model (Bi et al., 2013a, ACCESS-CM;) output, are carried out for the output from an ACCESS ocean–sea-ice model (ACCESS-OM; Bi et al., 2013b) simulation forced with prescribed atmospheric conditions and bulk formulae of Large and Yeager (2009) following the Coordinated Ocean-ice Reference Experiment phase 2 Inter-annual Forcing (CORE-II IAF) protocols as described in Griffies et al. (2012) (Table 1). Following Danabasoglu et al. (2014), we use the fifth cycle of a CORE-II IAF simulation for the analysis of ACCESS-OM presented here. Note that the ACCESS-OM simulation ends in 2007 which is the last year of CORE-II IAF.

The ACCESS-CM and ACCESS-OM configurations share the ocean and sea-ice models and by analysing their differences we can assess the role of the prescribed atmospheric forcing in driving changes in the Antarctic sea-ice concentration. The sea-ice model of ACCESS is the LANL Community Ice CodE version 4.1 (Hunke and Lipscomb, 2010), which uses the elastic-viscous-plastic rheology, and the ocean model is an implementation of the 2009 public release of the NOAA/GFDL MOM4p1 community code (Griffies et al., 2009). Both ACCESS-CM and ACCESS-OM use an identical horizontal discretisation on an orthogonal curvilinear tripolar grid with a nominal one degree resolution having additional refinements in the Arctic, in the Southern Ocean, and near the Equator. The ACCESS-CM atmospheric model has a horizontal resolution of 1.25° latitude by 1.875° longitude. ACCESS-OM is forced by CORE forcing with spherical T62 resolution (approximately 1.9°), although many meteorological variables, such as winds, are based on the NCEP/NCAR reanalysis with a coarser horizontal resolution of 2.5° latitude × 2.5° longitude.

There is a significant difference in the computation of sea-ice surface energy balance between ACCESS-CM and ACCESS-OM. As described in Bi et al. (2013a) ACCESS-CM has a semi-implicit atmospheric boundary layer that requires determination of the surface

Table 1
Model experiments used in this study.

Name	Years	Short description and reference
historical	1850–2005	Historical simulations that use evolving forcing such as volcanoes, aerosols, greenhouse gas concentrations and land use changes (Taylor et al., 2012)
rcp85	2005–2100	A future projection simulation forced with specified concentrations (RCPs), consistent with a high emissions scenario (Taylor et al., 2012)
CORE-II IAF	1948–2007	The second phase of The Coordinated Ocean-ice Reference Experiments (COREs) that uses inter-annually varying prescribed atmospheric forcing (IAF) of Large and Yeager (2009) under the experimental protocols introduced in Danabasoglu et al. (2014)

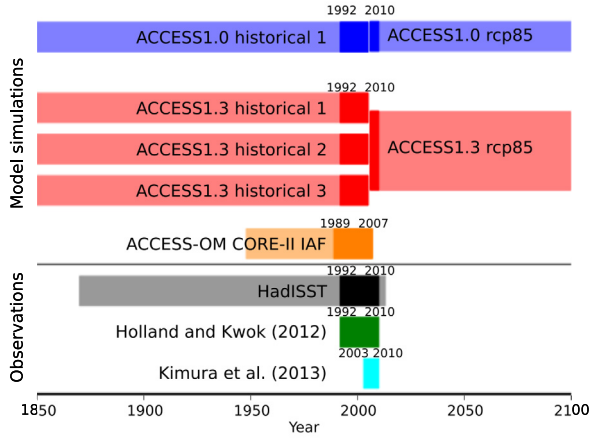

Fig. 1. Horizontal bars illustrate total time extent of model simulations and observations used in this study. Time periods selected for the analysis are highlighted with non-transparent colours with the start and end years written, while time periods excluded from the analysis are shown with transparent, fainter colours. (For interpretation of the references to colour in this figure legend, the reader is referred to the web version of this article.)

heat flux using a zero-layer thermodynamic calculation following Semtner (1976). In contrast, ACCESS-OM uses a 4-layer sea-ice thermodynamic discretisation that allows for a more realistic internal sea-ice temperature profile. In the multi-layer thermodynamic approach (ACCESS-OM), the sea-ice temperatures and net top and basal surface heat fluxes are together calculated iteratively, with a heat capacity that depends on internal material properties. The simpler zero-layer approach (ACCESS-CM) only accounts for top and basal sea-ice temperatures and assumes a linear internal sea-ice temperature profile with no heat capacity. As shown by Cheng et al. (2008), an increased number of sea-ice layers results in more realistic sea-ice thermodynamics. Despite this difference, having both ACCESS-CM CMIP5 and ACCESS-OM CORE-II simulations available is clearly an asset for our evaluation that is not available for many climate models.

Following Holland and Kwok (2012), we compute April–October (from 1 April to 31 October) daily sea-ice concentration budgets for ACCESS-CM realisations and for the ACCESS-OM experiment as,

$$\frac{\partial A}{\partial t} + \mathbf{u}\cdot\nabla A + A\nabla\cdot\mathbf{u} = f - r, \tag{1}$$

based on daily sea-ice concentration (A) and velocity ($\mathbf{u}$). The concentration change from freezing minus melting (f), and the concentration change from mechanical ice redistribution processes (r), such as ridging and rafting, are resolved as a residual component ($f - r$). In general, and in the Antarctic in particular, where the sea-ice drift tends to be divergent, the magnitude of f can be expected to be much larger than that of r.

Next, daily sea-ice concentration budgets are integrated over the April–October period for each year. The integral of the first term from the left in (1) provides the net change in the sea-ice concentration from the beginning to end of the period. The integral of the second term in (1) is the contribution to the sea-ice concentration change by the advection, the integral of the third term is the contribution by the divergence and the integral on the right hand side is the net contribution by the thermodynamic and ridging processes. After reorganising, the integrated ice concentration budget can be represented as,

$$\int_{t1}^{t2}\frac{\partial A}{\partial t}dt = -\int_{t1}^{t2}\mathbf{u}\cdot\nabla A dt - \int_{t1}^{t2}A\nabla\cdot\mathbf{u}dt + \int_{t1}^{t2}(f-r)dt, \tag{2}$$

where we denote the term on the left hand side of (2) as difference or *dadt*; the first term on the right hand side as advection or *adv*; the second term as divergence or *div*; and the third term as residual or *res*. Accordingly, the integrated budget and its components can be expressed compactly as

$$dadt = adv + div + res. \tag{3}$$

It is important to understand that the three components on the right hand side of (3) are interdependent and, for example, regions experiencing large rates of divergence are likely to experience ice growth under cold atmospheric conditions. Another example would be a case where the ice melt decreases the sea-ice concentration and thickness, and consequently results in a faster moving sea ice, which in turn affects the divergence and advection.

Finally, integrated components of sea-ice concentration budget are used to compute their average values over 19-year periods of 1992–2010 (ACCESS-CM) and 1989–2007 (ACCESS-OM). These periods were selected because they are as close as possible to the observational results covering 1992–2010, which is the longest period with reliable sea-ice concentration budget observations available (Holland and Kwok, 2012). The observed sea-ice concentration budget was calculated on a 100×100 km^2 grid, which has a resolution close to the ACCESS model grid (nominally 1°latitude $\times$ 1°longitude). Following Holland and Kwok (2012), we apply a low pass filter, where every grid point is replaced by the mean value of a 9-cell square centred on that point, on *adv*, *div*, and *res* in (3) to ensure the comparability of the model output with the observations. Model based results are robust and rather similar with or without the smoothing, but Holland and Kwok (2012) observation based results require smoothing to reduce grid-scale noise in the derivatives. Note that to cover the whole 1992–2010 period we joined four ACCESS-CM *historical* simulations, which end in 2005, with the *rcp85* simulation from 2006–2010 resulting in four combinations of time series — one combination for ACCESS1.0 and three for ACCESS1.3 (Fig. 1). To quantify the similarity between the observed and modelled sea ice, the normalised root-mean-square-error (NRMSE) was computed between the observed and modelled sea-ice concentration. We also compare the modelled sea-ice area, computed as the area integral of ice concentration, with the sea-ice area based on observational HadISST

data (Rayner et al., 2003), and we assess the agreement of modelled ice drift with a 2003–2010 ice velocity climatology computed from observation based data (Kimura et al., 2013). Kimura et al. (2013) have recently published a daily ice velocity product on a 37.5 km resolution grid which is prepared using the satellite passive microwave sensor Advanced Microwave Scanning Radiometer for EOS (AMSR-E) data over years 2003–2011.

3. Results and discussion

3.1. General characteristics

Monthly climatologies of Antarctic sea-ice extent, area and concentration derived from ACCESS simulations and the HadISST observational product are presented in Figs. 2 and 3. The sea-ice extent is defined as the integral of grid cells areas where the sea-ice concentration is larger than 15%. The sea-ice area is computed as the integral of grid cells areas multiplied by the sea-ice concentration in each grid cell. ACCESS-OM and ACCESS1.0 simulations have lower than observed April sea-ice extents, areas and concentrations in contrast to ACCESS1.3 April sea-ice extents, areas and concentrations which are close to and higher than observed, respectively. In October, ACCESS-CM sea-ice extents and areas are slightly higher than observed (Fig. 2) while ACCESS-CM sea-ice concentrations are lower than observed in the Weddell Sea and in the Ross Sea (Fig. 3). The ACCESS-OM sea-ice extent (area), however, is significantly higher (lower) than observed in October (Fig. 2). As shown in Fig. 3(f), the ACCESS-OM sea-ice concentration is low everywhere resulting in the too low sea-ice area, while the sea-ice extends too far off the coast of East Antarctica between 40°E and 110°E contributing to the too high sea-ice extent. Differences between October and April sea-ice areas are significantly larger in ACCESS1.0 simulations ($12.7–12.9 \times 10^6$ km^2) than observed (9.9×10^6 km^2), and close to the observed in ACCESS1.3 and ACCESS-OM simulations, being 9.5–9.9 and 9.5×10^6 km^2, respectively.

The evolution of sea-ice extent and area from April to October varies considerably between ACCESS simulations. The April–August sea-ice extent and area increases in the ACCESS-OM simulation and particularly in the ACCESS1.0 appear high, because their April sea-ice extents and areas are lower than observed and their August sea-ice extents and areas are close to or higher than observed (Fig. 2). ACCESS1.3 simulations have close to the observed sea-ice area increase from April to September and its sea-ice area remains higher than observed. As a result, both ACCESS-CM model configurations produce too high sea-ice area maxima in September although their sea-ice extents remain close to the observed. This indicates that, on the average, the winter ACCESS-CM sea-ice concentration is higher than observed. After September, the Antarctic sea ice starts to retreat and ACCESS-CM sea-ice extents decrease at observed rates, but ACCESS-CM sea-ice areas decrease at higher rates than observed until October. This discrepancy is due to the thinner than observed ACCESS-CM sea ice in the central ice pack, where the ice melt impacts the sea-ice area rather than the sea-ice extent, and is manifested as a lower than observed sea-ice concentration (Fig. 3(g) and (h)). The faster than observed September–October retreat indicate that the modelled sea ice responds to the atmospheric or oceanic forcing too strongly during these months.

The ACCESS-OM sea-ice extent peaks in September, while its sea-ice area peaks in August. This is due to the too thin ACCESS-OM sea ice in the central ice pack, which starts melting in August while the sea ice is still expanding northwards driven by CORE-II IAF atmospheric states. Because the average ACCESS-OM sea-ice concentration is lower than observed, the September ACCESS-OM sea-ice area is lower than observed even when its sea-ice extent is higher than observed. To understand more in detail which processes are driving the evolution of ACCESS sea ice, we next explore to which extent the April–October evolution of sea ice is driven by its dynamical and thermodynamical components.

Holland and Kwok (2012) computed the components of sea-ice concentration budget in wintertime (April–October) satellite data from 1992–2010 when the Antarctic sea-ice cover experiences its seasonal northward expansion (Figs. 2 and 4(a)). During the expansion, the sea-ice concentration increases from zero to close to 100% in the ice pack around the continent, especially in longitudes 20°W–30°E in the Weddell Sea, as the ice edge advances northward (Fig. 4(a)). The advection of sea ice contributes to the autumnal increase of sea-ice concentration mainly along the northernmost perimeter of the maximum sea-ice area (Fig. 4(b)). The divergent ice motion in the central ice pack decreases the ice concentration, which then, under low air temperatures, enhances the thermodynamic ice growth and increases the ice concentration (Fig. 4(c) and (d)).

In some limited coastal regions, such as east of the Antarctic Peninsula and along the coast of the western Ross Sea, the ice converges and the residual component is negative (Fig. 4(c) and (d)). It

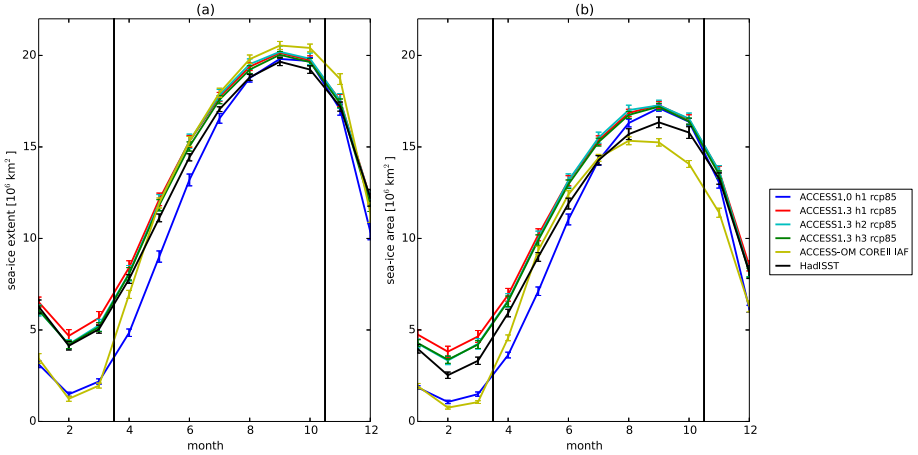

Fig. 2. Monthly mean sea-ice (a) extent and (b) area climatologies derived from observational HadISST data and ACCESS model output. HadISST and ACCESS-CM climatologies are based on 1992–2010 time period, while the ACCESS-OM climatology is based on 1989—2007 time period. Vertical bars indicate 95% confidence limits of monthly means. The beginning of April and the end of October are marked with black vertical lines. Sea-ice extent is the integral of grid cells areas where the sea-ice concentration is larger than 15%, while sea-ice area is the area integral of ice concentration.

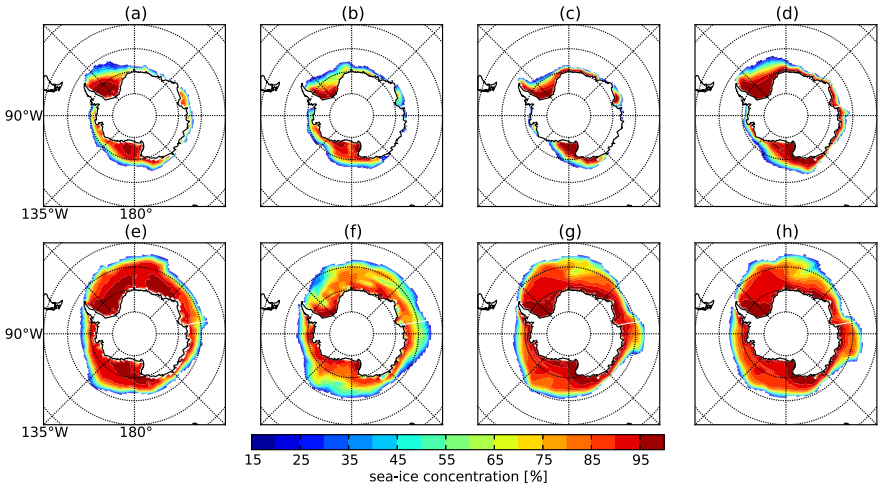

Fig. 3. April (a)–(d) and October (e)–(h) mean sea-ice concentration for (a,e) HadISST from 1992–2010, (b,f) ACCESS-OM from 1989–2007, (c,g) ACCESS1.0 ensemble from 1992–2010 and (d,h) ACCESS1.3 ensemble from 1992–2010.

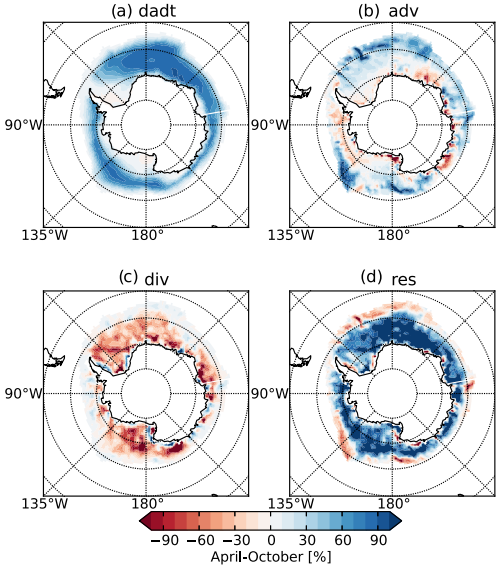

Fig. 4. April–October 1992–2010 mean of each component in the ice concentration budget based on observational SSM/I data (Holland and Kwok, 2012).

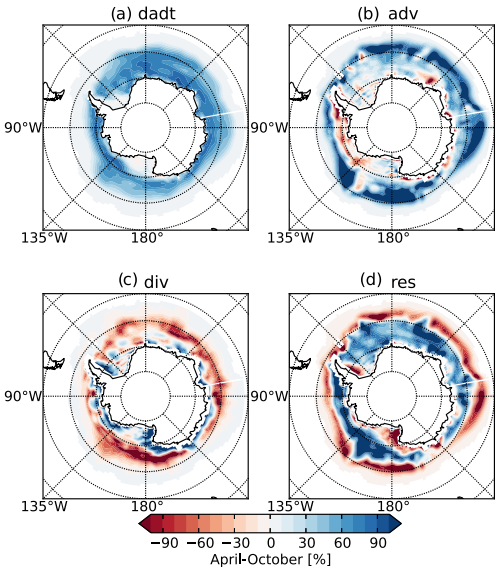

Fig. 5. April–October 1989–2007 mean of each component in the ice concentration budget based on the ACCESS-OM CORE-II IAF simulation.

should be noted here that the Holland and Kwok (2012) observational sea-ice concentration budget does not allow us to consider these regions nearest to the coast where large rates of divergence and freezing occur in autumn and winter. We can not calculate the divergence ($\nabla \cdot \mathbf{u}$) there from the observational data, because the ice velocity near the coastline has a significant sub-pixel geometry, so to call one pixel 'land' and ascribe the zero flow there is potentially incorrect — hence $\nabla \cdot \mathbf{u}$ remains unknown. Moreover, ∇ is highly uncertain since the coastline is poorly resolved. However, we can calculate $\nabla \cdot \mathbf{u}$ over larger regions next to the coast, although not at the pixel scale. Therefore the Holland and Kwok (2012) approach can only really show the sea-ice divergence and the residual term on the large scale and on finer scales in the inner pack away from the coast. The model output does not have this issue, but regions at the immediate vicinity of the coast can not be compared between model based and observation based results, and were not included in the analysis.

Another region where the residual component is negative is at the northern limit of Antarctic sea-ice extent, where the ice melts after being advected into these warm regions (Fig. 4(b) and (d)). Hence, even though the residual component is generally positive, indicating the dominance of thermodynamical processes because ridging cannot create ice area, it can become negative under certain circumstances — when the ice is compressed and ridging deformation occurs, or when the ice melts. Overall, the observed sea-ice concentration budget provides an insightful picture of the roles of the various physical processes contributing to the autumn–winter evolution of Antarctic sea ice and is a valuable diagnostic tool.

3.2. Simulations with prescribed atmosphere

Mean components of the ACCESS-OM CORE-II IAF sea-ice concentration budget are shown in Fig. 5. General features of April–October rate of sea-ice concentration change agree with observations (compare Fig. 5(a) with Fig. 4(a)). The increase in sea-ice concentration occurs in the band extending from the Weddell Sea around East Antarctica, the Ross Sea and the Amundsen Sea to the Bellingshausen Sea. In the southern Weddell Sea and the

southern Ross Sea the ice concentration is similar in both the ACCESS-OM simulation and in observations.

Despite similar general features between ACCESS-OM and observations, there are also significant differences, particularly in coastal regions, where the ACCESS-OM sea-ice concentration increases more than observed due to the fact that at the beginning of April the ACCESS-OM ice area is lower than observed (Fig. 2). This results in a broader than observed band of sea-ice concentration increase (Fig. 5(a)). On the contrary, the ACCESS-OM ice concentration increases less than observed in the Weddell Sea and in the Pacific Sector, from 170°E to 90°W, which is the reason why the September ACCESS-OM sea-ice area remains lower than observed (Fig. 2).

The ACCESS-OM and observations disagree at the northernmost edge of the sea ice. The ACCESS-OM April–October ice concentration change is higher than observed around East Antarctica where the ice is advected too far north (Figs. 4(b) and 5(b)). In the northern Weddell Sea, the ACCESS-OM residual term is too small due to a combination of strong advection and weak divergence (Figs. 4 and 5), and results in a negative bias in the ACCESS-OM April–October ice concentration change. Hence, although some general features of ACCESS-OM ice advection match with observations — the ice is transported from the coastal regions, where the advection decreases the ice concentration, to the north where the ice concentration increases (Figs. 4(b) and 5(b)) — the ACCESS-OM ice advection results in positive ice concentration biases close to the edge of the maximum ice extent, which are indicated in the residual component as excessive melting (Fig. 5(d)). We further note that the large north–south gradients in the residual term partly originate from the fact that the mean for April–October is only calculated on the basis of the sub-period when there is sea ice in a certain region; the northernmost regions are not affected by the autumn freezing.

In the central ice pack and close to the coast, the ACCESS-OM sea-ice divergence values are largely offset by values of the residual component (Fig. 5(c) and (d)). In coastal regions, the convergent ice motion positively contributes to ice concentration, but away from the coast the opposite occurs as the divergent ice motion decreases the ice concentration. As seen in Fig. 4(c), the Antarctic ice motion is mainly divergent and the (coastal) area of convergent motion is very small according to observations. In the ACCESS-OM simulation, however, the area of convergent motion is much larger and correspondingly the observed area of divergent motion is much smaller (Fig. 5(c)). This is associated with the fact that the ACCESS-OM residual component is quite different than observed, as seen from Fig. 5(d), where the blue area, signifying the thermodynamic growth of ice, is much smaller than observed (Fig. 4(d)). Accordingly, two and very likely interdependent biases are obvious: the ACCESS-OM coastal ice drift is too convergent; and the areas of thermodynamic growth are too limited and near the coast overtaken by the mechanical deformation.

Although the April–October ice concentration change appears similar in ACCESS-OM and in observations, contributions by the advection, the divergence and the residual component are notably different. A significant part of the difference between ACCESS-OM and observations is due to the ice motion, namely the extensive convergence near the coast and too strong advection off the coast in ACCESS-OM. This is due to too high ACCESS-OM ice velocities, as we show at the end of this section. The simulation of sea ice in the Southern Ocean is sensitive to wind forcing and its resolution especially along the Antarctic coast (Stössel et al., 2011). Because the surface wind is the most important factor driving the ice drift, inaccuracies in the CORE-II IAF atmospheric states are likely to deviate the modelled ice drift from observed and explain part of the disagreement. The prescribed reanalysis atmospheric state tends to constrain the modelled sea-ice extent to that observed because reanalysis atmospheric surface variables are impacted by observed surface conditions including the sea-ice concentration and the sea surface temperature.

It is important to note that biases in the divergence and in the residual component largely balance each other resulting in a relatively realistic seasonal evolution of sea-ice concentration which is driven by advection to a larger degree than is observed. The lack of thermodynamic growth is more apparent in the ice thickness than ice concentration and the ACCESS-OM ice remains too thin partly because the ice velocity is excessively fast, and the ice thus advances north too early and partly because of a warm and overly convective Southern Ocean which is typical for the ACCESS model and for other ocean–ice models (Bi et al., 2013b; Griffies et al., 2009; Marsland et al., 2003). Model parameterisations also play an important part and can be used, for example, to adjust the sea-ice evolution via heat conductivity, the air-ice momentum drag coefficient, the ice-ocean stress turning angle and the mechanical deformation rates (Uotila et al., 2012). In this paper we have found evidence that it is not enough to adjust the model by selecting a set of parameter values that reproduce a realistic looking ice concentration distribution, or area or extent, but the best set of model parameters should produce as realistic looking components of sea-ice concentration budget as possible. Therefore we emphasise the importance of model velocity assessment against those observed.

Area integrals of sea-ice concentration budget components summarise how each component impacts the evolution of sea-ice area from April to October (Table 2). The ACCESS-OM April–October sea-ice area change is 1.6×10^6 km^2 larger than the observed mainly because the ACCESS-OM April sea-ice area is lower than observed (Fig. 2). The ACCESS-OM ice advection is more than three times stronger than observed and is the dominant component in the sea-ice concentration budget. The ACCESS-OM ice is advected into regions where the prescribed CORE-II IAF near surface air temperatures are low enough that ice does not melt, but as the modelled advection is too strong, the ice advances north too soon and remains thin. The combined impact of divergence and residual components in ACCESS-OM is much smaller than observed (0.2×10^6 km^2 compared to 6.1×10^6 km^2). The small difference between the divergence and residual component further highlights the fact that these two components counterbalance in ACCESS-OM, and as a result the ACCESS-OM April–October sea-ice area change is close to observed despite being dominated by advection. The thermodynamics of sea-ice melt and freeze determine in-situ production and destruction of sea ice while the dynamical processes of advection and divergence redistribute existing sea ice. The thermodynamic and dynamic processes are tightly coupled, so that the strong sea-ice advection biases identified in the ACCESS models also manifest as strong biases in the thermodynamic term.

The ACCESS model uses the elastic-viscous-plastic rheology which causes ice to response more sensibly to the wind than the classical viscous-plastic rheology, particularly when the ice concentration is higher than 0.9 (Massonnet et al., 2011). In the Antarctic, the ice motion is generally divergent and the role of rheology is smaller than in the Arctic, and, as Massonnet et al. (2011) conclude, the model skill is not limited due to model physics, but due to other factors such as model resolution and atmospheric forcing.

It is possible that the ACCESS-OM air-ice drag coefficient is too large under stably stratified conditions (which prevail over sea ice). This is not due to aerodynamic roughness length, which is as low as 0.005 m in ACCESS-OM, but due to the fact that the model applies a function (Holtslag and de Bruin, 1988) that reduces the drag coefficient with stability much less than most other experimental functions (Andreas, 1998). It is also possible that, due to the prescribed atmospheric states that drive the ACCESS-OM sea

Table 2
Area integrals of Antarctic April–October ice concentration budget mean components in 10^6 km^2 and in parenthesis as percentages of *dadt*. For ACCESS1.0 and ACCESS1.3 ensemble minimum and maximum values are listed.

Name	dadt	adv	(%)	div	(%)	res	(%)
Holland and Kwok (2012)	9.4	3.3	(35)	−5.0	(−53)	11.1	(118)
ACCESS-OM	11.0	10.8	(98)	−3.0	(−27)	3.2	(29)
ACCESS1.0	13.1–13.3	15.7–16.1	(121)	−6.5 to −6.2	(−48)	3.6–3.7	(27)
ACCESS1.3	10.1–10.6	15.4–15.9	(151)	−9.1 to −8.4	(−85)	3.3–3.5	(34)

ice, important atmosphere–ocean feedback mechanisms that would modify the atmosphere and further impact the sea-ice concentration budget in a fully coupled model, are missing. Therefore we discuss next how sea-ice concentration budgets in fully coupled ACCESS-CM simulations compare with the ACCESS-OM sea-ice concentration budget and with the observed budget.

3.3. Coupled simulations

Components of the ACCESS-CM April–October sea-ice area change are shown in Table 2. The April–October sea-ice area change is larger than observed in ACCESS-CM due to the slightly too high October sea-ice area, and particularly in ACCESS1.0 due to its low April sea-ice area (Fig. 2). As with ACCESS-OM, the ice advection dominates the sea-ice area budget, almost five times larger than the observed. Contrary to the ACCESS-OM divergence, the area integrals of ACCESS-CM divergence are more negative than the area integral of the observed divergence. Hence, the ACCESS-CM ice drift is more divergent and the relative importance of divergence is larger in the ACCESS-CM sea-ice concentration budget (from −85% to −48%, Table 2) than in the ACCESS-OM sea-ice concentration budget (−27%, Table 2). ACCESS-CM residual components are much smaller than observed and, as with ACCESS-OM, are associated with the very large positive values of the ice advection in the sea-ice concentration budget. Hence, although the April–October sea-ice area change is relatively close to the observed in ACCESS-CM, its components are very different from observed.

How well then do the modelled sea-ice concentration budget components agree with observed components and is the ACCESS-OM sea-ice concentration budget more realistic than the ACCESS-CM sea-ice concentration budget? We address these questions quantitatively by using the NRMSE metric. As seen in Table 3, metrics for $dadt$, adv, div and res are similar for ACCESS-CM and ACCESS-OM simulations. Additionally, within the ACCESS-CM ensemble biases and metrics vary very little (Tables 2 and 3) and the multi-layer sea-ice thermodynamics scheme of ACCESS-OM does not cause better NRMSE compared to ACCESS-CM. Therefore, ACCESS-OM and ACCESS-CM sea-ice concentration budgets appear equally unrealistic.

In addition to area integrals of sea-ice concentration budget components, it is important to look at how sea-ice concentration budgets vary across the Antarctic region in ACCESS-CM simulations. The ACCESS-CM sea-ice concentration budget components based on the ensemble member that agrees best with observations according to Table 3 are shown in Fig. 6. Although the general advection pattern looks reasonable in the ACCESS-CM simulation, as was the case for ACCESS-OM, the ice is advected along the boundary of the maximum ice extent at much higher rates than observed (compare Figs. 6(b) and 4(b)). Regarding the ACCESS-CM divergence, the regions of convergence are not as extensive as in the ACCESS-OM simulation, but still more widespread than in observations (compare Figs. 4(c), 5(c) and 6(c)). Additionally, ACCESS-OM has lower rates of sea-ice divergence and residual term in the central ice pack than ACCESS-CM. However, the melting of sea ice along the boundary of the maximum sea-ice extent, which is larger than observed, reduces the area integral of the ACCESS-CM residual component. Hence, the main reason for the disagreement between the ACCESS-CM sea-ice concentration budget and the observed sea-ice concentration budget is too strong ice advection in ACCESS-CM near the ice edge, and the excessive convergence near the coast. A common factor of these model-observation disagreements is the ice drift, which we analyse in the next section.

Table 3
NRMSE between modelled April–October sea-ice concentration budget mean components and observed April–October 1992–2010 sea-ice concentration budget mean components of Holland and Kwok (2012). For ACCESS 1.0 and ACCESS1.3 ensemble minimum and maximum values are listed. All correlation coefficients have p-values less than 0.05.

	ACCESS-OM	ACCESS1.0	ACCESS1.3
dadt	0.21	0.29	0.20–0.22
adv	0.08	0.11	0.10–0.11
div	0.11	0.10	0.11
res	0.11	0.13	0.13

Before analysing the ice drift we check how well the residual term corresponds to the sea-ice thermodynamics. This is possible because the ACCESS-CM simulation output includes the water flux into the ocean due to melting and freezing of sea ice (Fig. 6(e)). Although the water flux output is available as monthly means and the residual term is based on daily data, the spatial agreement between the ACCESS-CM residual (Fig. 6(d)) and the water flux due to thermodynamics is very good with regions of freezing (negative water fluxes) matching the positive regions of the residual term in the central ice pack and regions of melting matching the negative regions of the residual term close to the ice edge. An exception is that in regions of convergent ice drift (western Weddell Sea, southwestern Ross Sea, and a tongue further west of the latter; Fig. 6(c)), the residual term (Fig. 6(d)) does not match with the fresh water flux (Fig. 6(e)). Please note here that the ice loss in the residual term near the western sides of the Weddell and Ross seas is therefore from convergence and ridging, which thickens the ice at the expense of ice area, as proposed by Holland and Kwok (2012). Hence, our comparison supports the interpretation of Holland and Kwok (2012) that the residual term provides a good representation of the thermodynamic variability.

3.4. Ice drift

It has become apparent that the main reason for disagreement of ice concentration budget between ACCESS and observations is the higher than observed ice advection in ACCESS, and, as shown in Eq. (1), the main factor affecting the ice advection is the drift speed. Consistent with the strong advection, the mean April–October ice speed simulated by ACCESS is about two times higher than the observational speed of Kimura et al. (2013). Hence, the reason for the strong advection in ACCESS is the high drift speed.

Fig. 7 highlights the regional differences between observations, ACCESS-OM and ACCESS-CM. The coastal drift is too strong in ACCESS and while impacting the advection it also generates the strong convergence zone where the ice concentration increases (Figs. 7, 5(c) and 6(c)). The extensive zone of convergence could

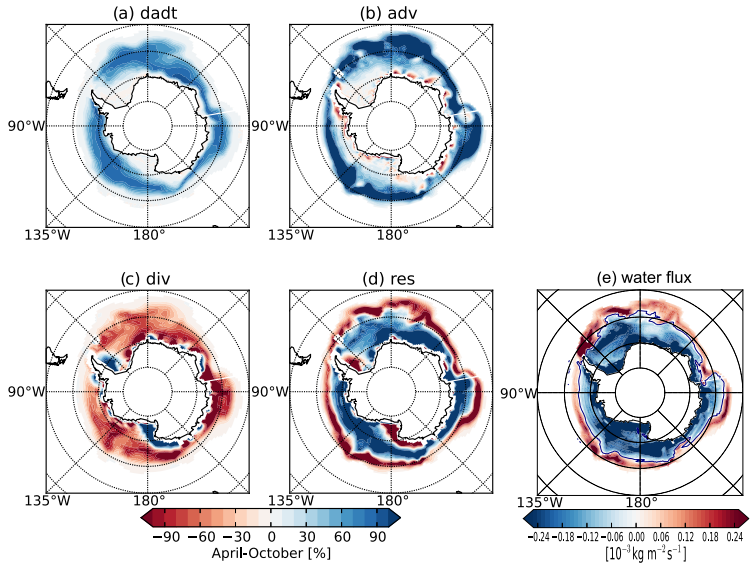

Fig. 6. (a)–(d) April–October 1992–2010 mean of each component in the ice concentration budget based on the merged ACCESS1.3 historical ensemble member 1 and rcp85 simulations. (e) April–October 1992–2010 mean of the fresh water flux into the ocean due to freezing (negative flux) or melting (positive flux) of sea ice for the same simulations. This ensemble member rather than other members is plotted because it has the lowest NRMSE (*dadt*) with respect to the (Holland and Kwok, 2012) observations.

partly be a result of a relatively coarse ocean–ice model grid, ranging from 0.25° at 78°S to 1° at 30°S, which does not resolve the coastal velocities with the adequate accuracy. In addition, a high atmospheric resolution is required to resolve winds which push newly formed sea ice away from the coast. The CORE-II IAF winds are based on the NCEP/NCAR reanalysis and, as shown by Stössel et al. (2011), an ocean–ice model forced with horizontal resolution of 2.5° latitude ×2.5° longitude NCEP/NCAR winds produces three times less sea ice along the coast than the same model forced with 0.225° × 0.225° high resolution winds. It is likely that even the 1.875° × 1.25° horizontal resolution of ACCESS-CM atmosphere is not high enough to resolve the coastal wind field and increase the sea-ice production.

In the central ice pack, such as in the central Weddell Sea, in the Ross Sea and in the Amundsen–Bellingshausen Seas, the ACCESS ice speed is relatively close to observed, but the direction of ACCESS ice velocity somewhat differs from the observed velocities, particularly in the Weddell Sea where the ACCESS ice velocity has a stronger westward component than observed (Fig. 7). North of the central ice pack, at the northernmost edge of the sea ice, the ACCESS ice velocities are much higher than observed. It is certain that the regions of higher-than-observed ice speed, close to the coast and at the ice edge, deviate the ACCESS ice concentration budget from observed. These are, however, the regions where the estimates of observed ice velocities are most uncertain which increases uncertainties of the sea-ice concentration budget components.

It is clear that in Fig. 5(d) and in 6(d) the ice growth is reasonable in the pack (dark blue), so the low mean value of the residual term (Table 2) is coming from the excessive red near the coast and at the ice edge. We have confirmed that the negative residual near the coast is due to excessive ridging, which must be from excessive velocity near the coast. It also seems highly likely that the excessive melting near the ice edge is simply compensating excessive advection into that region. In that sense the thermodynamics are wrong and they have been adjusted to melt away the excessive ice flux towards the ice edge.

However, we still think the root cause of the problem is the dynamics. How could excessive melting near the ice edge cause excessive advection (vdA/dy) towards the ice edge? It is possible that an excessive dA/dy could contribute but given that we have shown that v is far too large that seems like the obvious culprit. Hence, it seems very likely that there is an excessive advection which is bringing more ice into the melting zone and distorting the thermodynamics.

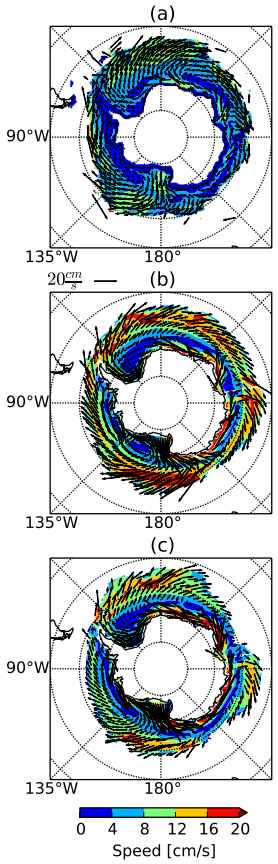

Fig. 7. (a) 2003–2010 April–October mean ice velocity vectors and mean ice speed contour plot based on observational data of Kimura et al. (2013), (b) 1989–2007 ACCESS-OM CORE-II IAF April–October mean ice velocity vectors and speed, and (c) as (b), but based on the merged 1992–2010 ACCESS1.3 historical ensemble member 1 and rcp85 simulations.

4. Conclusion

ACCESS models simulate the overall seasonal evolution of Antarctic sea-ice extent and area realistically, but with contributions from the components of the sea-ice concentration budget that significantly differ from contributions based on observations of Holland and Kwok (2012). Accordingly, we accept our research hypothesis that climate models simulate the seasonal evolution of integrated Antarctic sea-ice area, and integrated extent, reasonably well, even with relatively unrealistic dynamic and thermodynamic components of the sea-ice concentration budget, mainly due to the balancing of biases of these components. ACCESS models agree best with observations in the central ice pack and disagree close to the Antarctic coast and at the ice edge. Because these are the regions where the observation based estimates of ice drift are most uncertain, it is reasonable to conclude that the true sea-ice concentration budget is somewhere between model and observation based estimates.

The sea-ice concentration budget proved to be a valuable model diagnostic tool for three reasons. First, the observation based estimates of Holland and Kwok (2012) provide a very reasonable decomposition of the roles of the various physical processes contributing to the autumn–winter evolution of Antarctic sea ice and the integrated sea-ice area. Second, we showed that the sea-ice concentration budget is sensitive to model configurations when we compared differences between ACCESS-CM configurations and ACCESS-OM, and therefore it seems that models can effectively be adjusted to reproduce the sea-ice concentration budget components as realistically as possible. To further highlight this sensitivity, we carried out an additional ACCESS-OM simulation (not described above), otherwise identical to the one analysed in this study, but instead of zero ice–ocean stress turning angle the simulation used a 16° ice–ocean stress turning angle. As a consequence, the contribution of advection to sea-ice area decreased to half and the contribution of the thermodynamics increased about 50%, but the contribution of divergence changed from negative to positive being clearly unrealistic. Third, contributions of sea-ice concentration budget components to the sea-ice area and regional evolution of sea ice are generally similar in ACCESS-OM and ACCESS-CM. This indicates that, at least to some extent, the model adjustments required for the simulation of as realistic sea-ice concentration budget components as possible can be carried out by using a computationally cheaper ocean–sea-ice model instead of a fully coupled model.

Specifically, our sea-ice concentration budget analysis revealed the strong advection and the widespread coastal convergence in ACCESS due to the faster than observed ice drift, which causes the simulated sea-ice concentration budget to deviate from the observed. This erroneous balance of terms is important for the oceanic processes — if the ice comes from advection rather than freezing, then the sea-ice volume remains low and the ocean will feel only a fraction, in our case one third, of the salt flux that it should receive. This reduced salt flux might help to explain the oceanic warm bias in models, for instance. Importantly, in order to reproduce the observed Antarctic sea-ice extent trend, models have to be able to simulate the sea-ice concentration budget realistically and therefore the ice drift and coastal convergence should be key focus areas of model assessment and development.

Acknowledgments

This research was funded by the Academy of Finland through the AMICO project (Grant 263918) and by the Australian Government Department of the Environment, the Bureau of Meteorology and CSIRO through the Australian Climate Change Science Programme. This work was supported by the NCI National Facility at the ANU. We thank the ACCESS model development team for producing and making available their model output.

References

Andreas, E.L., 1998. The atmospheric boundary layer over polar marine surfaces. In: Leppäranta, M. (Ed.), Physics of Ice-Covered Seas, vol. 2. Helsinki University Printing House, Helsinki, pp. 715–773.

Bi, D., Dix, M., Marsland, S.J., O'Farrell, S., Rashid, H., Uotila, P., Hirst, A., Kowalczyk, E., Colebiewski, M., Sullivan, A., Hailin, Y., Hannah, N., Franklin, C., Sun, Z., Vohralik, P., Watterson, I., Zhou, X., Fiedler, R., Collier, M., Ma, Y., Noonan, J., Stevens, L., Uhe, P., Zhu, H., Hill, R., Harris, C., Griffies, S., Puri, K., 2013a. The ACCESS coupled model: description, control climate and evaluation. Aust. Meteorol. Oceanogr. J. 63 (1), 41–64.

Bi, D., Marsland, S.J., Uotila, P., O'Farrell, S., Fiedler, R., Sullivan, A., Griffies, S.M., Zhou, X., Hirst, A.C., 2013b. ACCESS-OM: the ocean and sea-ice core of the ACCESS coupled model. Aust. Meteorol. Oceanogr. J. 63 (1), 213–232.

Cheng, B., Zhang, Z., Vihma, T., Johansson, M., Bian, L., Li, Z., Wu, H., 2008. Model experiments on snow and ice thermodynamics in the Arctic Ocean with CHINARE2003 data. J. Geophys. Res. 113, C09020. http://dx.doi.org/10.1029/2007JC004654.

Danabasoglu, G., Yeager, S.G., Bailey, D., Behrens, E., Bentsen, M., Bi, D., Biastoch, A., Böning, C., Bozec, A., Cassou, C., Chassignet, E., Danilov, S., Diansky, N., Drange, H., Farneti, R., Fernandez, E., Fogli, P.G., Forget, G., Gusev, A., Heimbach, P., Howard, A., Griffies, S.M., Kelley, M., Large, W.G., Leboissetier, A., Lu, J., Maisonnave, E., Marsland, S.J., Masina, S., Navarra, A., George Nurser, A.J., y Mélia, D.S., Samuels, B.L., Scheinert, M., Sidorenko, D., Terray, L., Treguier, A.-M., Tsujino, H., Uotila, P., Valcke, S., Voldoire, A., Wang, Q., 2014. North Atlantic Simulations in coordinated ocean-ice reference experiments phase II (CORE-II). Part I: Mean states. Ocean Modell., 76–107. http://dx.doi.org/10.1016/j.ocemod.2013.10.005.

Dix, M., Vohralik, P., Bi, D., Rashid, H., Marsland, S.J., O'Farrell, S., Uotila, P., Hirst, A.C., Kowalczyk, E., Sullivan, A., Yan, H., Franklin, C., Sun, Z., Watterson, I., Collier, M., Noonan, J., Rotstayn, L., Stevens, L., Uhe, P., Puri, K., 2013. The ACCESS coupled model documentation of core CMIP5 simulations and initial results. Aust. Meteorol. Oceanogr. J. 63 (1), 83–99.

Griffies, S., Biastoch, A., Boning, C., Bryan, F., Danabasoglu, G., Chassignet, E., England, M., Gerdes, R., Haak, H., Hallberg, R., Hazeleger, W., Jungclaus, J., Large, W.G., Madec, G., Pirani, A., Samuels, B.L., Scheinert, M., Sen Gupta, A., Severijns, C.A., Simmons, H.L., Treguier, A.M., Winton, M., Yeager, S., Yin, J., 2009. Coordinated ocean-ice reference experiments (COREs). Ocean Modell. 26 (1–2), 1–46.

Griffies, S.M., Winton, M., Samuels, B., Danabasoglu, G., Yeager, S., Marsland, S., Drange., H., Bentsen, M., 2012. Datasets and protocol for the CLIVAR WGOMD coordinated ocean-sea ice reference experiments (COREs). WCRP Report No. 21/2012, p. 21.

Holland, P.R., Kwok, R., 2012. Wind-driven trends in Antarctic sea-ice drift. Nat. Geosci. 5 (11), 1–4. http://dx.doi.org/10.1038/ngeo1627.

Holland, P.R., Bruneau, N., Enright, C., Losch, M., Kurtz, N., Kwok, R., 2014. Modelled trends in Antarctic sea ice thickness. J. Clim. http://dx.doi.org/10.1175/JCLI-D-13-00301.1.

Holtslag, A.A.M., de Bruin, H.A.R., 1988. Applied modeling of the nighttime surface energy balance over land. J. Appl. Meteorol. 37, 689–704.

Hunke, E.C., Lipscomb, W.H., 2010. CICE: the Los Alamos sea ice model documentation and software users manual. LA-CC-06-012 Tech. Rep., 176.

Kimura, N., Nishimura, A., Tanaka, Y., Yamaguchi, H., 2013. Influence of winter sea ice motion on summer ice cover in the Arctic. Polar Res. 32, 20193. http://dx.doi.org/10.3402/polar.v32i0.20193.

Large, W.G., Yeager, S.G., 2009. The global climatology of an interannually varying air-sea flux data set. Clim. Dyn. 33, 341–364. http://dx.doi.org/10.1007/s00382-008-0441-3.

Liu, J., Song, M., Horton, R.M., Hu, Y., 2013. Reducing spread in climate model projections of a September ice-free Arctic. Proc. Natl. Acad. Sci.. http://dx.doi.org/10.1073/pnas.1219716110.

Mahlstein, I., Gent, P.R., Solomon, S., 2013. Historical Antarctic mean sea ice area, sea ice trends, and winds in CMIP5 simulations. J. Geophys. Res.: Atmos. 118, 1–6. http://dx.doi.org/10.1002/jgrd.50443.

Marsland, S.J., Haak, H., Jungclaus, J.H., Latif, M., Röske, F., 2003. The Max-Planck-Institute global ocean/sea ice model with orthogonal curvilinear coordinates. Ocean Modell. 5 (2), 91–127. http://dx.doi.org/10.1016/S1463-5003(02)00015-X.

Massonnet, F., Fichefet, T., Goosse, H., Vancoppenolle, M., Mathiot, P., Beatty, C.K., 2011. On the influence of model physics on simulations of Arctic and Antarctic sea ice. Cryosphere 5, 1167–1200. http://dx.doi.org/10.5194/tcd-5-1167-2011.

Massonnet, F., Mathiot, P., Fichefet, T., Goosse, H., König Beatty, C., Vancoppenolle, M., Lavergne, T., 2013. A model reconstruction of the Antarctic sea ice thickness and volume changes over 1980–2008 using data assimilation. Ocean Modell. 64, 6775. http://dx.doi.org/10.1016/j.ocemod.2013.01.003.

Meier, W.N., Gallaher, D., Campbell, G.G., 2013. New estimates of Arctic and Antarctic sea ice extent during September 1964 from recovered Nimbus I satellite imagery. Cryosphere 7 (2), 699–705. http://dx.doi.org/10.5194/tc-7-699-2013.

Polvani, L.M., Smith, K.L., 2013. Can natural variability explain observed Antarctic sea ice trends? New modeling evidence from CMIP5. Geophys. Res. Lett.. http://dx.doi.org/10.1002/grl.50578.

Rayner, N.A., Parker, D.E., Horton, E., Folland, C.K., Alexander, L.V., Rowell, D., Kent, E., Kaplan, A., 2003. Global analyses of sea surface temperature, sea ice, and night marine air temperature since the late 19th century. J. Geophys. Res. 108 (D14), 4407. http://dx.doi.org/10.1029/2002JD002670.

Semtner, A.J., 1976. A model for the thermodynamic growth of sea ice in numerical investigations of climate. J. Phys. Oceanogr. 63, 79–389.

Solomon, S., Qin, D., Manning, M., Chen, Z., Marquis, M., Averyt, K.B., Tignor, M., Tignor, M., Miller, H.L. (Eds.), 2007. Climate Change 2007: The Physical Science Basis. Contribution of Working Group I to the Fourth Assessment Report of the Intergovernmental Panel on Climate Change. IPCC (2007) Summary for Policymakers. Cambridge University Press, Cambridge, UK, New York, NY, USA.

Stössel, A., Zhang, Z., Vihma, T., 2011. The effect of alternative real-time wind forcing on Southern Ocean sea ice simulations. J. Geophys. Res. 116, C11021. http://dx.doi.org/10.1029/2011JC007328.

Swart, N.C., Fyfe, J.C., 2013. The influence of recent Antarctic ice sheet retreat on simulated sea ice area trends. Geophys. Res. Lett. 40, 4328–4332. http://dx.doi.org/10.1002/grl.50820.

Taylor, K.E., Stouffer, R.J., Meehl, G.A., 2012. An overview of CMIP5 and the experiment design. Bull. Am. Meteorol. Soc. 93, 485–498. http://dx.doi.org/10.1175/BAMS-D-11-00094.1.

Turner, J., Comiso, J.C., Marshall, G.J., Lachlan-Cope, T.A., Bracegirdle, T.J., Maksym, T., Meredith, M.P., Wang, Z., Orr, A., 2009. Non-annular atmospheric circulation change induced by stratospheric ozone depletion and its role in the recent increase of Antarctic sea ice extent. Geophys. Res. Lett. 36 (8), 1–5. http://dx.doi.org/10.1029/2009GL037524.

Turner, J., Bracegirdle, T.J., Phillips, T., Marshall, G.J., Hosking, J.S., 2013a. An initial assessment of Antarctic sea ice extent in the CMIP5 models. J. Clim. 26 (5), 1473–1484. http://dx.doi.org/10.1175/JCLI-D-12-00068.1.

Turner, J., Phillips, T., Hosking, J.S., Marshall, G.J., Orr, A., 2013b. The Amundsen Sea low. Int. J. Climatol. 33 (7), 1818–1829. http://dx.doi.org/10.1002/joc.3558.

Uotila, P., O'Farrell, S., Marsland, S.J., Bi, D., 2012. A sea-ice sensitivity study with a global ocean-ice model. Ocean Modell. 51, 1–18, j.ocemod.2012.04.002.

Uotila, P., O'Farrell, S., Marsland, S.J., Bi, D., 2013a. The sea-ice performance of the Australian climate models participating in the CMIP5. Aust. Meteorol. Oceanogr. J. 61 (1), 121–143.

Uotila, P., Vihma, T., Tsukernik, M., 2013b. Close interactions between the Antarctic cyclone budget and large-scale atmospheric circulation. Geophys. Res. Lett. 40, 1–5. http://dx.doi.org/10.1002/grl.50560.

Zhang, J., 2013. Modeling the impact of wind intensification on Antarctic sea ice volume. J. Clim.. http://dx.doi.org/10.1175/JCLI-D-12-00139.1.

Zunz, V., Goosse, H., Massonnet, F., 2013. How does internal variability influence the ability of CMIP5 models to reproduce the recent trend in Southern Ocean sea ice extent? Cryosphere 7 (2), 451–468. http://dx.doi.org/10.5194/tc-7-451-2013.